NeuroImage 201 (2019) 116032

Contents lists available at ScienceDirect

NeuroImage

journal homepage: www.elsevier.com/locate/neuroimage

Color contrast adaptation: fMRI fails to predict behavioral adaptation

Erin Goddard, Dorita H.F. Chang [1], Robert F. Hess, Kathy T. Mullen [*]

McGill Vision Research, Department of Ophthalmology, McGill University, Montreal, QC, H3G1A4, Canada

ARTICLE INFO

Keywords:
BOLD adaptation
S-cone isolating
Koniocellular
Color vision
Temporal scales

ABSTRACT

fMRI-adaptation is a valuable tool for inferring the selectivity of neural responses. Here we use it in human color vision to test the selectivity of responses to S-cone opponent (blue-yellow), L/M-cone opponent (red-green), and achromatic (Ach) contrast across nine regions of interest in visual cortex. We measure psychophysical adaptation, using comparable stimuli to the fMRI-adaptation, and find significant selective adaptation for all three stimulus types, implying separable visual responses to each. For fMRI-adaptation, we find robust adaptation but, surprisingly, much less selectivity due to high levels of cross-stimulus adaptation in all conditions. For all BY and Ach test/adaptor pairs, selectivity is absent across all ROIs. For RG/Ach stimulus pairs, this paradigm has previously shown selectivity for RG in ventral areas and for Ach in dorsal areas. For chromatic stimulus pairs (RG/BY), we find a trend for selectivity in ventral areas. In conclusion, we find an overall lack of correspondence between BOLD and behavioral adaptation suggesting they reflect different aspects of the underlying neural processes. For example, raised cross-stimulus adaptation in fMRI may reflect adaptation of the broadly-tuned normalization pool. Finally, we also identify a longer-timescale adaptation (1h) in both BOLD and behavioral data. This is greater for chromatic than achromatic contrast. The longer-timescale BOLD effect was more evident in the higher ventral areas than in V1, consistent with increasing windows of temporal integration for higher-order areas.

1. Introduction

Contrast adaptation allows the visual system to maximize its dynamic range across changing environments and is an example of a normalization process that increasingly appears to be ubiquitous in neural processing. Adaptation has also commonly been used as a tool in visual neuroscience to infer the tuning of distinct visual responses. In human color vision, psychophysical studies of contrast adaptation have been used to infer the number and tuning of the chromatic and achromatic mechanisms. Selective adaptation indicated the existence of three separable mechanisms (luminance, L/M cone opponent and S-cone opponent) that adapt largely independently (Krauskopf et al., 1982, 1986). Although at suprathreshold contrasts, adaptation suggests that the two color axes are combined into a wider range of chromatic responses (Webster and Mollon, 1994). These studies helped form the basis of a "cardinal" color space that has been extensively used over the ensuing decades.

Subsequent work has used fMRI adaptation to compare the within- and cross-stimulus effects of adaptation to isoluminant red-green (RG) and achromatic (Ach) contrast (Chang et al., 2016; Engel, 2005; Engel and Furmanski, 2001; Mullen et al., 2015). In each of these cases, adaptation to either RG or Ach contrast produced both selective and unselective adaptation effects. In area V1, Engel and Furmanski (2001) found evidence of selective adaptation to RG stimuli but not Ach stimuli. Mullen et al. (2015), however, did not find selective adaptation to either RG or Ach stimuli in V1, but instead found selective adaptation emerged in higher-level ventral cortical areas for RG contrast and in dorsal areas for Ach contrast, reflecting the differential specializations of these two pathways, although significant cross-adaptation always remained.

Here, we extend this result in a series of fMRI adaptation experiments designed to measure the selectivity of the S-cone opponent (BY) responses in relation to Ach and RG contrast. We measure within-stimulus and cross-stimulus adaptation across a range of visual areas between the two-color processes (BY and RG), and between the achromatic (Ach) and BY processes. RG/Ach adaptation was excluded as it has previously been reported (Mullen et al., 2015). We then compare the fMRI BOLD results with measurements of psychophysical contrast adaptation for both a threshold detection task and a suprathreshold measure of perceived contrast using the same stimuli as in the BOLD experiment, but with timing closer to that used in previous psychophysical work. For our BOLD

* Corresponding author.
E-mail address: kathy.mullen@mcgill.ca (K.T. Mullen).
[1] Current address: Department of Psychology, The University of Hong Kong.

https://doi.org/10.1016/j.neuroimage.2019.116032
Received 1 March 2019; Received in revised form 4 June 2019; Accepted 17 July 2019
Available online 18 July 2019

results, we find no evidence for selectivity between the BY and Ach processes, with similar cross- and within-stimulus adaptation for the BY adaptation of Ach test stimuli as well as Ach of BY. This compares to the selectivity of the RG contrast response from Ach in ventral cortex, and of Ach from RG in dorsal cortex, found previously (Mullen et al., 2015). For the chromatic pairs, we also find a trend for selectivity in ventral cortex. In contrast, our psychophysical experiments show a very different pattern of results, with high stimulus selectivity for all stimulus pairs. Interestingly, the psychophysical experiments reveal subtly different adaptation effects for the threshold and suprathreshold conditions in terms of the cross-stimulus adaptation effects for these mechanism-isolating stimuli. Overall, we conclude that that BOLD adaptation results do not reflect the perceptual effects, implying different aspects of the neural processes underlie BOLD and behavioral adaptation. In addition, the uniformly high levels of cross-stimulus adaptation between the BY and Ach contrasts are surprising in the light of the psychophysical results and known physiological findings. Finally, we also considered the timescale over which adaptation effects accumulate. For both fMRI BOLD and the psychophysical measures, we find evidence that adaptation continues to accumulate across a 1h session, particularly for chromatic stimuli, and for the BOLD responses in higher cortical areas.

2. Materials and methods

2.1. Participants

A total of 19 unique participants (12 female, age range 20–35) were tested across the two fMRI experiments. 12 observers were tested in each of Experiment 1 (7 female, mean age = 27.8) and Experiment 2 (7 female, mean age = 26.8). For the psychophysical experiments (Experiments 3 and 4), a total of 12 unique participants were tested, including 4 participants who took part in one or both fMRI experiments. Ten observers were tested in each of Experiments 3 (7 female, mean age = 29.9), and 4 (7 female, mean age = 26.9). All participants were healthy with no history of neurological and/or psychiatric disorders and provided informed consent. Each participant had normal or corrected-to-normal visual acuity, and normal color vision as assessed with Ishihara plates (Ishihara, 1990) and the Farnsworth-Munsell 100-hue test (Farnsworth, 1957). All experiments were approved by the Ethics Review Board of the McGill University Health Centre and were conducted in accordance with the Declaration of Helsinki.

2.2. Visual stimuli

For both fMRI and psychophysical experiments the stimuli were radial sinewave gratings (0.5 cycles/degree) with 2 Hz sinusoidal contrast phase alternation, as used in previous work (Mullen et al., 2007, 2015). The ring contrast was either achromatic (Ach), isoluminant 'red-green' (RG) or 'blue-yellow' (BY), modulated about a mean gray, isolating the luminance, L/M cone opponent and S-cone mechanisms respectively (Fig. 1). The low spatial frequency of the stimuli reduces luminance artifacts generated by chromatic aberration for the chromatic stimuli (Bradley et al., 1992; Cottaris, 2003; Mullen, 1985). The stimulus diameter was 15° and a small fixation marker was displayed in the centre (a black dot). Across all experiments, the adapting and test stimuli had the same spatio-temporal parameters, except in the case of the contrast matching psychophysical experiment (Experiment 4), in which test stimuli were divided into two halves (as depicted in Fig. 1), with the left and right halves consisting of wedges of the ring stimulus (angular width 144°) with their edges smoothed using a cosine spatial envelope over an angular width of 3°.

Stimulus chromaticities were defined in a three-dimensional cone contrast space, with each axis representing the quantal catch of the L, M and S cone types normalized with respect to the gray background (i.e. cone contrast). The vector direction and length within this space defines chromaticity and cone contrast respectively. We determined

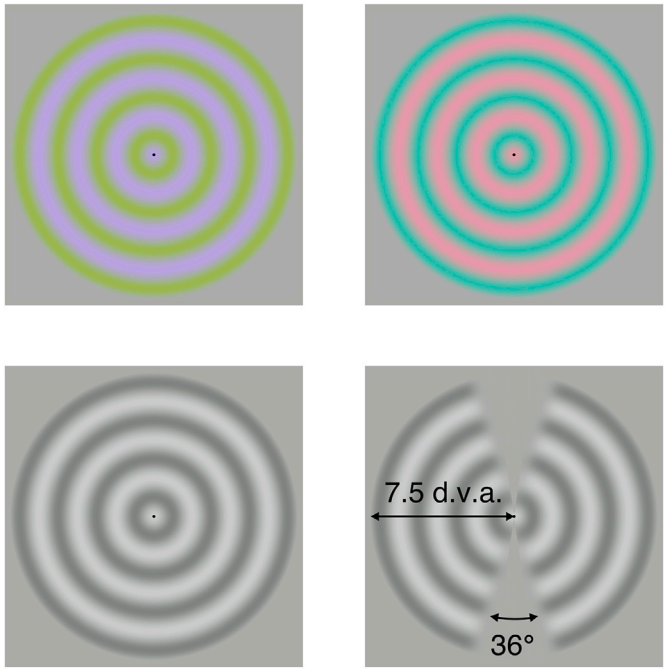

Fig. 1. Visual stimuli. In both the fMRI and psychophysical experiments, the visual stimuli were radial sinewave gratings isolating the S-cone (top left), L/M cone opponent (top right), or luminance (bottom left) mechanisms, shown at higher contrast in these illustrations than in the experiments. The spatial layout was the same across experiments, except in Experiment 4, where stimuli had the layout depicted in the bottom right.

isoluminance of the RG stimuli for each subject individually based on perceptual minimum motion settings as previously described (Mullen et al., 2007, 2010). We also verified the angle of the BY mechanism within each participant's isoluminant plane by varying vector angle and selecting the direction of minimum visibility (Michna et al., 2007).

Across Experiments 1-4, the adapting stimuli had cone contrasts of 22% (Ach, ~20 x detection threshold), 1.8% (RG, ~10 x detection threshold) or 11.6% (BY, ~10 x detection threshold). These contrasts were chosen to yield stimuli that, importantly, evoked robust BOLD responses of similar amplitudes in previous work (Mullen et al., 2010) and in pilot data. Although these criteria resulted in achromatic stimuli that may have been more salient, all stimuli were highly visible, and we preferred to equate the stimuli in the BOLD responses they evoked. We confirmed that stimuli of these contrasts evoked BOLD responses of similar magnitude in the no-adaptation condition (Figure S1), except in hMT+, for which chromatic stimuli were excluded from further analysis (see below). In the fMRI experiments (Experiments 1 and 2) these contrasts were used for both the adapting and test stimuli, and in Experiment 4 they were used for the reference stimuli.

2.3. Display apparatus and calibrations

For 10 participants in Experiment 1 we back-projected the stimuli on a screen using a LCD projector (NEC VT580, resolution 1024 x 768, frame rate 60 Hz, mean luminance 270 cd/m^2). For the remaining two participants in Experiment 1 and for all participants in Experiment 2 we displayed stimuli on a 32" BOLD screen LCD monitor (Cambridge Research Systems Ltd, Rochester, UK, resolution 1920x1080, refresh rate 60Hz, mean luminance 52.4 cd/m^2). Participants viewed the back-projected image or BOLD screen, which was located at the rear of the MRI bore, through a mirror mounted on the head coil. The total viewing distance was 125 cm. We used a Macbook Pro (2015) running Matlab (R2017a) in conjunction with routines from Psychtoolbox 3.0 (Brainard, 1997; Kleiner et al., 2007; Pelli, 1997) to generate the stimuli and draw them to

the projector or screen. For Experiments 3 and 4, and for preliminary testing to determine isoluminance, we used Matlab R2006a in combination with a VSG 2/5 graphics board with 14 bits of contrast resolution (Cambridge Research Systems Ltd, Rochester, UK) housed in a Pentium PC and displayed on a CRT monitor (Diamond Pro, 2070). The BOLD screen, LCD projector and the CRT display were each linearized and color calibrated as described previously (Michna et al., 2007; Mullen et al., 2007).

2.4. fMRI methods: experimental design

For the fMRI experiments, participants viewed repeating cycles of an adapting stimulus (12s), test stimulus (18s) and fixation stimulus (9s) (Fig. 2), as described in previous work (Chang et al., 2016; Mullen et al., 2015). Adapting and test stimulus pairs were BY and RG in Experiment 1 and BY and Ach in Experiment 2. For each experiment, there were two sessions of scanning on separate days with different adaptors used on different days. Each participant completed four 8-min runs in each session; each run commenced with an initial 9s fixation block, followed by 12 repeats of the adapt/test/fixate cycle. On half of these cycles, the adapting stimulus was replaced with a gray screen to acquire a no-adaptation condition. Across the four 8-min runs, we collected 12 repeats of the 2 test stimuli paired with the adaptor, and 12 repeats of the same test stimuli paired with the no-adaptation condition. We counterbalanced the order in which the adaptor and test pairs were presented across runs, and we varied the order of the two sessions with different adapting stimuli across participants.

Throughout the 12s adapting stimulus block, the stimulus constantly contrast-reversed over time at 2Hz with sinusoidal temporal modulation. During each 18s test stimulus block, the participants were instructed to fixate on the central marker and performed 6 trials of a 2IFC contrast-discrimination task, as used previously (Mullen et al., 2007, 2010, 2015). During each 3s trial, the ring stimulus was presented twice with a near-threshold contrast difference between them (a 15% contrast increment added to one stimulus and a 15% decrement to the other, yielding a 30% contrast difference about the mean contrast). Each stimulus was presented within a Gaussian temporal envelope (sigma 125 ms, total duration 500 ms), with a 500 ms ISI. In the remaining trial time (1.5s) the participants indicated with a button press which interval contained the higher contrast stimulus. During the fixation stimulus participants also completed a contrast discrimination task (3 trials in each 9s block) on a half cycle of the Ach ring stimulus that surrounded the fixation dot.

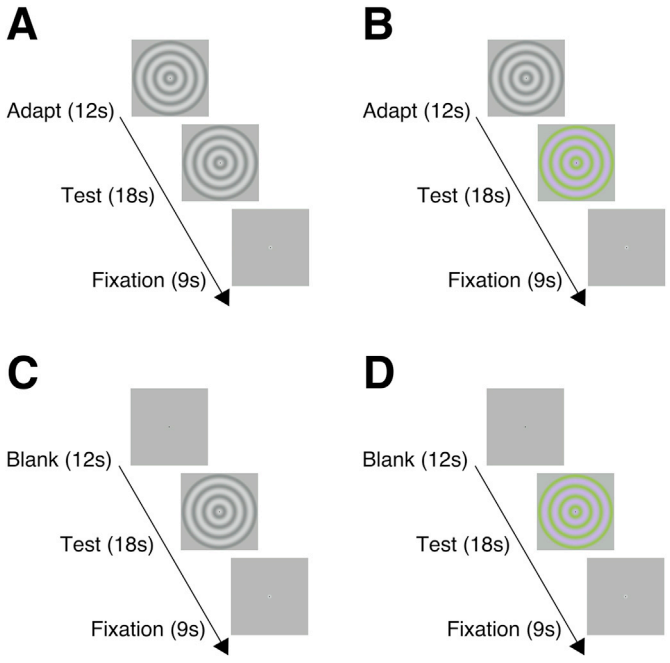

Fig. 2. Example stimulus cycles from fMRI experiments. The fMRI experiments consisted of repeating cycles of the adapting stimulus (12s), test stimulus (18s), and fixation stimulus (9s). For an example (Ach adaptor) session, the Ach adaptor could be presented before an Ach test stimulus (**A**: within-stimulus adaptation), or a BY test (**B**: cross-stimulus adaptation), or the adapting stimulus could be blank and followed by an Ach (**C**) or BY (**D**) test stimulus.

2.5. fMRI methods: retinotopic and functional localizers

We identified the visual cortical regions V1, V2, V3, V3A/B, LO1/LO2 and hV4 for each participant using rotating wedge stimuli and expanding and contracting concentric rings (Engel et al., 1994; Sereno et al., 1995), following standard definitions of these areas (Goddard et al., 2011; Larsson and Heeger, 2006; Wandell et al., 2005). To localize areas VO1 and VO2 we used data from the retinotopic mapping scans in conjunction with a VO localizer, based on this region's higher sensitivity for chromatic over achromatic cone contrast (Mullen et al., 2007). To compare each voxel's responsiveness to chromatic and achromatic contrast, we used RG and Ach ring stimuli of the same spatial and temporal properties as for the adaptation experiment equated in cone contrast (average of 3.55%). Participants performed the same contrast discrimination task as described above for 6 trials (18s) interleaved with 3 trials (9s) of the fixation task, repeated over 12 blocks. Each participant completed at least 2 runs of the VO localizer. Coordinates of each participant's VO1 and VO2 are shown in Table S1.

To localize hMT+ we used a localizer stimulus similar to that described previously (Huk et al., 2002). In a block design, participants viewed 10s blocks of moving and static dots, interspersed with blank intervals (also 10s duration). Moving and static dot stimuli were comprised of 2000 low contrast dots (10% contrast, half luminance increments and half luminance decrements, each with a circular spatially smoothed Gaussian envelope with radius 0.33°) on a background of mean gray luminance. Blank blocks consisted of a mean gray screen. During moving blocks, the dots moved smoothly towards or away from fixation at 8.4°/*s*, with direction alternating at 1Hz. In static blocks, randomly selected frames from the moving stimulus were presented, updated at 1Hz. Participants were instructed to maintain fixation on a central marker and performed a simple task at fixation. During retinotopic mapping scans, participants used a button press to report the direction of a small arrow that appeared for 400ms at a rate of ~1Hz, with temporal jittering. During the hMT+ localizer participants indicated when the fixation marker changed from light to dark gray.

Retinotopic mapping stimuli were presented within a central square of the display, of width 17.5° visual angle, and the area outside of the stimulus was black. For the hMT+ localizer the moving/static dot locations were restricted to an annulus (inner diameter 3.5°, outer diameter 15.7°) and the remaining screen was mean gray. All participants completed at least 4 repeats of the 6-min rotating wedge stimulus (2 with clockwise and 2 with counter-clockwise rotation), and 1 or 2 6-min scans with an expanding/contracting ring stimulus. Each participant completed 1 or 2 repeats of the 7.5-min hMT+ localizer.

2.6. fMRI methods: scanning protocols

All magnetic resonance imaging took place at the McConnell Brain Imaging Centre (Montréal, Canada). Functional T2* MR images were acquired on a 3T Siemens MAGNETOM Prisma system with 32-channel head coil. Gradient-echo pulse sequences were used to measure blood oxygenation level-dependent (BOLD) signal as a function of time. For the earlier scans (data from the first 10 participants for Experiment 1, and the retinotopic mapping scans for these participants) we used a scanning protocol with coverage of the whole head (TR = 3000 ms, TE = 30 ms, 44 axial slices, 3.0 mm^3 resolution). For later scans (the remaining 2 participants of Experiment 1, all data from Experiment 2, and the retinotopic mapping scans for these participants) we used a scanning protocol with

partial head coverage (including the entire occipital cortex, with slices oriented parallel to the calcarine sulcus), but a finer spatial resolution (TR = 3000 ms, TE = 30 ms, 39 axial slices, 1.5 mm^3 resolution). Localization of hMT+ was performed in a separate scan with a multiband acceleration factor of 3 (39 axial slices, 1.5 mm^3 resolution, TR = 1210 ms, TE = 30.4 ms). Head movement was limited by foam padding within the head coil. For each participant, we acquired two high-resolution three-dimensional T1 images using an MP-RAGE sequence (TI = 900 ms, TR = 2300 ms, TE = 3.41 ms, 1.0 mm^3 resolution), and averaged these two images to generate the participant's anatomical template.

2.7. fMRI analysis: surface definition and preprocessing of functional data

For each participant's anatomical template, we used the automatic segmentation processes from Freesurfer 6.0 (Dale et al., 1999) to define the gray/white matter and pial/gray matter boundaries. For all other MRI data processing, we used AFNI/SUMA packages (AFNI 17.2.12, Sep 6, 2017; Cox, 1996; Saad et al., 2004). All functional data were pre-processed using slice-time correction and rigid-body motion correction before being aligned to the participant's anatomical template. Functional data were then projected onto the cortical surface by averaging between the white and pial boundaries, spatially smoothed (Gaussian filter, full-width at half maximum of 4 mm), and then data for each surface node was scaled by the node's mean response across the run. Converting functional data to a surface-based space (nodes) from a physical space (voxels) before smoothing reduces spatial distortions that would be introduced if smoothing across adjacent voxels that sample sections of cortex that are far apart on the cortical surface due to cortical folding (i.e. within a sulcus).

2.8. fMRI analysis: general linear modeling (GLM)

Data collected during the phase-encoded retinotopic mapping scans (rotating wedge and expanding ring) were analyzed using a Fourier analysis of response phase (Saad et al., 2001). For all the remaining functional data (VO localizer, hMT+ localizer, and data from the adaptation experiments) BOLD responses were modelled using the AFNI script *3dDeconvolve* which, in addition to stimulus-related regressors, included regressors for linear and polynomial trends and 6 motion correction parameters. Stimulus-related responses were extracted in terms of their beta amplitudes, equivalent to modelled percent signal change. For the VO localizer, we modelled the responses to RG and Ach blocks as single-parameter canonical BOLD responses (using 'BLOCK(18,1)' from *3dDeconvolve*), with the fixation blocks used as an implicit baseline. Similarly, for the hMT+ localizer we modelled responses to the moving and static blocks (using 'BLOCK(10,1)'). For the adaptation experiment, our model included estimates of the responses to two adapting stimuli (using 'BLOCK(12,1)') and to the different test stimuli (using 'BLOCK(18, 1)') in each adaptation condition, including separate estimates for each test stimulus paired with each adapting stimulus and for the no-adapt baseline responses to each test stimuli for different days of scanning.

To measure slower changes in the responses to test stimuli, for the adaptation experiment we also estimated responses using an alternate GLM. This alternate GLM included all the same regressors, except that we obtained separate response amplitude estimates for each stimulus presentation rather than obtaining a single estimate of average response for each stimulus type.

We visualized results from the phase-encoded retinotopic mapping scans and the VO and hMT+ functional localizers on inflated cortical representations using SUMA and used these data to define the regions of interest (V1, V2, V3, V3A, V3B, LO1, LO2, hV4, VO1, VO2 and hMT+) for each participant. Across participants, we were not always able to separate V3A from V3B, or LO1 from LO2, using retinotopic mapping data and so report data for a single, combined ROI in each case (V3A/B and LO).

2.9. fMRI analysis: measurement of adaptation effects

Using the general linear modelling from the adaptation experiment, we first selected surface nodes with stimulus-responsive voxels. We selected nodes with a greater response to the test stimuli following no-adaption blocks than to fixation, using a liberal criterion ($t_{(1109)} > 1.65$, $p < 0.10$, uncorrected). For each participant we then averaged the parameter estimates (beta values) across all stimulus-responsive nodes within each ROI. Across participants, the average response to the test stimuli in the no-adaptation baseline tended to be between 0.5 and 1 (beta value, equivalent to estimated percent signal change), as shown in Figure S1. An exception to this trend was hMT+, which had a low baseline response to RG and BY test stimuli (average beta: 0.2–0.3). Due to this low baseline response, we excluded hMT+ from our analyses of adaptation effects, except in the case of the Ach test.

To estimate the adaptation-related signal loss, we compared each ROI's response to a given test stimulus when preceded by the no-adaptation blank condition versus the adapting stimulus. To remove the effect of individual variations in participants' overall responses, (e.g. see Fig. 3B), we estimated the ratio of response to the test stimuli post-adaptation compared to no-adaptation by fitting a line to the scatter-plot of these ratios across participants. The lines were constrained to go through the origin, so had a single free parameter (*slope*). We defined the adaptation effect as 1 – *slope* since a slope of 1 indicates no difference between the two conditions. To estimate the 95% confidence intervals on these adaptation effect measurements, we generated a bootstrapped distribution of slope estimates for 10,000 samples of the data from the 12 participants (each sample comprised 12 values randomly selected from the original data, with replacement).

In a control analysis, we selected the half of our participants ($n = 6$) with the largest adaptation effects, averaged across within- and cross-stimulus adaptation and across ROIs. To select these participants we calculated each participant's average reduction in beta value, as a proportion of the response to the no-adaptation test stimulus. We then repeated the slope estimation and bootstrapping procedure for this smaller sample. To test whether these distributions of adaptation effect measurements were significantly above zero (one-sided test) we used the proportion of values below zero as a *p*-value, and applied a false discovery rate (FDR) criterion to correct for multiple comparisons (Benjamini and Hochberg, 1995).

We also used the bootstrapped distributions of adaptation effects to test for significant differences in adaptation effects across different adaptor stimuli, for each test stimulus in each ROI. For each of the 10,000 bootstrapped estimates of adaptation effects, we used the same random sampling with replacement for different adaptation/test stimulus combinations. To ask whether there were significant differences in these adaptation effects across adaptation stimulus conditions, we used the relevant samples to generate a distribution of 10,000 difference values. From this distribution and estimated the probability (*p*-value) that the mean of these difference values was different from zero (two-sided test) as the twice the proportion of values that were above zero (where the mean < 0) or below zero (where the mean > 0).

Similarly, we used the bootstrapped data to ask, for each ROI, whether there was a significant interaction between adaptation and test stimulus in the adaptation effects. For each ROI, we used the difference between the bootstrapped difference values for the 2 test stimuli (calculated above) to generate a distribution of estimates of the interaction. We then asked whether this interaction was significantly different from zero (two-sided test) by calculating *p*-values in a method analogous to above.

To estimate the signal loss caused by a slower timescale of adaptation of the response to the test stimulus, we used the data from the alternate GLMs described above. From these we obtained separate estimates for each of the 12 times each test stimulus was presented following a no-adaptation period during a single session. We used the no-adaptation periods alone so that for each participant we could average these

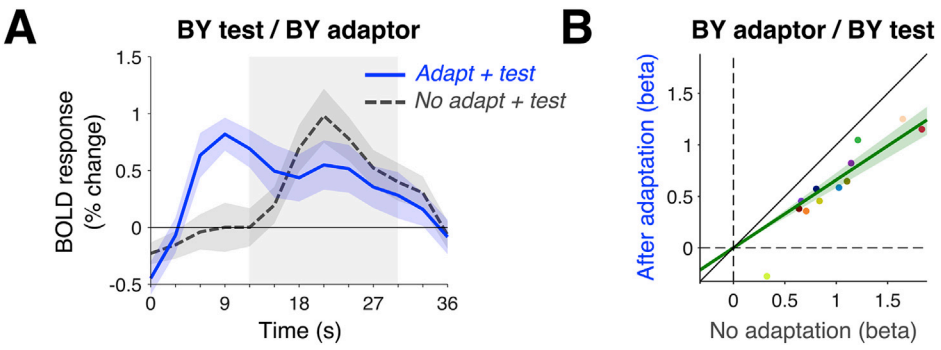

Fig. 3. Timecourses and adaptation effects for V1. **A**: Example timecourses from Experiment 2, for the BY test stimulus paired with a BY adaptor. The shaded gray background indicates the duration of the BY test stimulus presentation. The response to the test stimulus (peaking at ~21s) is of lower amplitude following the adapting stimulus (filled blue line) than following the no-adaptation blank screen (dashed line). Shaded error bars indicate the 95% confidence intervals of the between-subject mean ($n = 12$). **B**: For the same condition as in **A**, the estimates of response amplitudes from the GLMs are plotted. Each dot indicates data from a single participant. The line of best fit (thick green line) was of shallower slope that the unity line (thin black line). The green shaded region indicates the 95% confidence interval of the line of best fit (derived from bootstrapped estimates).

estimates across the two sessions (which included identical tests following no-adaptation periods but varied in their adaptor stimuli). This yielded 12 individual presentation estimates, where each is the average of 2 values. We then found the best-fitting line to relate response (beta value) to presentation number and defined the adaptation effect as the negative slope of this line for each participant's data. For each test stimulus, in each ROI, we normalized each participant's slope estimate by the mean response (beta value) across all presentations before averaging across participants. We tested whether these normalized adaptation effects were significantly above zero using a one-sided *t*-test on the between-subject mean.

2.10. Psychophysical experiments

We completed two psychophysical experiments (Experiments 3 and 4) to measure the perceptual effects of within-stimulus and cross-stimulus adaptation using the same visual stimuli. In Experiment 3 we measured the effects of adaptation on detection thresholds using a 2-interval forced choice (2IFC) task. In Experiment 4 we measured the suprathreshold effects of adaptation on perceived contrast using a 2-alternative forced choice (2AFC) task, with the same high contrasts for the adapting stimuli as used in the BOLD experiments. Stimuli for these experiments had the same contrast and spatiotemporal parameters as in the fMRI experiments, but the timing of the adaptation protocol was chosen to be closer to that used in previous psychophysical work (implications of this are considered below). For both Experiment 3 and 4, each participant completed the task for each of 3 test stimuli (Ach, RG and BY) in each of 4 adaptation conditions (no-adaptation baseline, adapt Ach, adapt RG and adapt BY). No-adaptation baseline data was acquired before any adaptation runs, and data using different adaptation stimuli were acquired on different days.

In the 2IFC detection task (Experiment 3), on each trial participants used a keypress to report whether the first or second interval contained a stimulus. Adaptation runs commenced with 60 s of adaptation, and between each trial there was 2 s of top-up adaptation, with a 0.5 s interval between the end of adaptation and the start of the first test stimulus. Each pair of test stimulus onsets were separated by 1 s, and the start of each interval was indicated by a tone. The mean gray background and central fixation marker were present through the experiment. Each test stimulus appeared within a Gaussian temporal envelope (sigma 125 ms, total duration 500 ms), and the screen remained gray until in the participant indicated their response, which triggered the onset of the next trial. The contrast of the test stimulus was varied using a 2-up 1-down staircase procedure: after 2 correct responses at a given contrast, the contrast was lowered by 10%, while after an incorrect response the contrast was increased by 20%. Each staircase was terminated after 6 reversals, with a reversal defined as an incorrect response following a correct response. For each condition we simultaneously acquired data for 2 staircases, with trials randomly interleaved. A run of the no-adaptation condition took ~5 min to complete, while a run including adaptation took approximately 10 min to complete. Each participant completed 2 runs (4 staircases) for each adaptor/test combination. The order in which data from the different test stimuli were acquired was counter-balanced across participants, but for each adapting stimulus the order of the 3 test stimuli in the first half of the session was reversed for the second half. Detection threshold was defined as the average of the contrasts at which reversals occurred.

In the 2AFC task (Experiment 4), the adapting and test stimuli had a modified spatial arrangement where the ring stimulus was divided into 2 parts, on the left and right of fixation (see Fig. 1, lower right). The adaptation protocol was similar to that used in Experiment 3: adaptation runs commenced with 60 s of adaptation, and between each trial there was 2 s of top-up adaptation, with a 0.5 s interval between the end of adaptation and the start of the test stimulus. On each trial, participants judged whether the stimulus on the left or the right was of higher contrast. Adapting stimuli were always restricted to one half (left or right) while the other half of the screen was held at mean gray, but were otherwise the same as in Experiment 3. On each trial, one part (left or right) contained a reference stimulus (Ach, RG or BY) of the same contrast as the corresponding adapting stimuli, while the stimulus on the other side (the test stimulus) was the defined by the same color direction as the reference but with contrast that was varied across trials using a 1-up 1-down staircase procedure. Each time the test stimulus was judged to be higher contrast than the reference its contrast was lowered by 20% of the reference contrast, while each time it was judged to be lower contrast its contrast was raised by 20% of the reference contrast. Staircases were terminated after 6 reversals (each reversal was a response of 'test higher contrast' following a response of 'test lower contrast'). Each run consisted of 4 interleaved staircases: 2 with the reference stimulus on the left and 2 with it on the right of fixation. As in Experiment 3, each participant completed 2 runs for each condition, the no-adaptation runs were acquired before any adaptation data, and the order of the test stimuli was counter-balanced across participants. The shift in point of subjectively equal contrast was defined as the average of the contrasts at which reversals occurred. In Experiment 4 there were 2 adaptation conditions for each stimulus color, one on the left and one on the right of fixation. We acquired data for each of these 6 adaptation stimuli on separate days.

To parallel the longer timescale analysis for the BOLD adaptation data, we also tested for slower adaptation effects in the psychophysical aftereffects. For both psychophysical experiments, the majority of participants completed each adaptation condition in a continuous session of ~1 h, so to test whether adaptation effects were building up over a longer timescale, we compared data collected in the first half of each session with data from the second half of each session (excluding participants who completed conditions across multiple sessions). By the second half of the session these participants had already completed at least half an hour

of testing, including at least 3 blocks of initial adaptation (60 s each) and ~300 trials, each with 2 s top-up adaptation.

3. Results

3.1. fMRI adaptation effects

Across visual cortex we found that responses to the test stimuli were lower following an adapting stimulus than following the no-adaptation blank screen. This is illustrated in Fig. 3 for an example stimulus (BY test with BY adaptor, from Experiment 2) in a single ROI (V1). The average voxel time-courses (Fig. 3A) illustrate the reduced response to the BY test stimulus following the adaptor, relative to the no-adaptation baseline. When the amplitudes of these responses were estimated using GLMs for each participant, there was a systematic decrease in amplitude following adaptation, as captured by the slope of the best-fitting line in Fig. 3B.

The adaptation effects (1 - *slope*) across all ROIs are shown in Fig. 4. Across most ROIs, we found robust signal loss for both within-stimulus adaptation and cross-stimulus adaptation for the chromatic pairs (Fig. 4A, BY and RG test stimuli combined with BY and RG adaptors), as well as for BY/Ach pairs (Fig. 4B, BY and Ach test stimuli combined with BY and Ach adaptors). We used the bootstrapped estimates of adaptation effects ($n = 10{,}000$ for each adapt/test combination) to test for

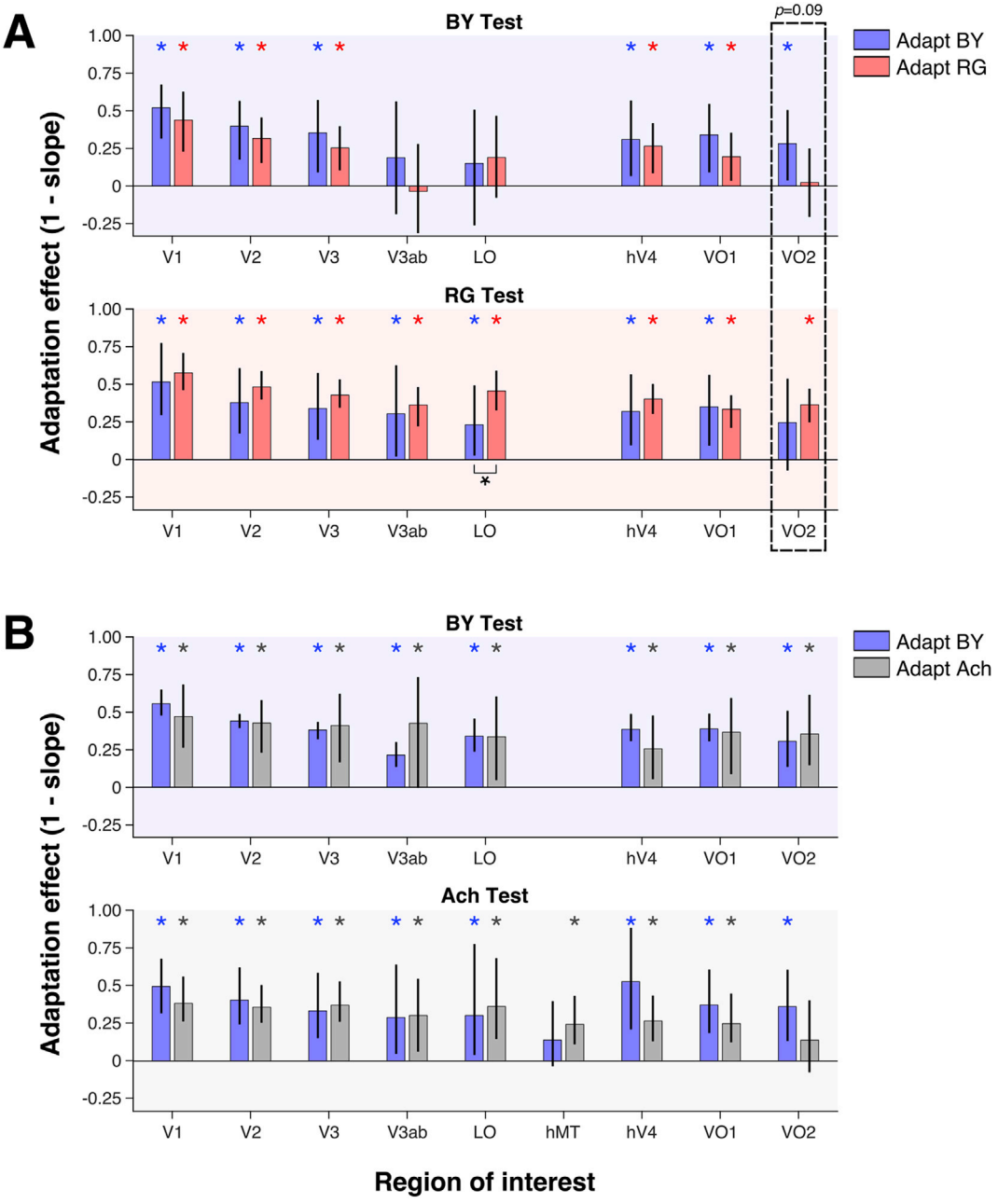

Fig. 4. Adaptation effects in: **(A)** Experiment 1, for the BY and RG test stimuli with BY and RG adaptors as marked and **(B)** Experiment 2, for the BY and Ach test stimuli with BY and Ach adaptors. In each plot, the adaptation effect is defined as 1 – *slope* where *slope* is the slope of the line of best fit across participants ($n = 12$), as illustrated in Fig. 3B. The error bars indicate the 95% confidence interval of the adaptation effect, as derived from bootstrapped estimates. Asterisks above the bars indicate cases where the adaptation effects were significantly greater than zero ($q < 0.05$, based on bootstrapped values, FDR corrected). A black asterisk indicates the one case (RG test, area LO) with a significant difference in adaptation effect between adaptors. Box with dashed line indicates the one case (VO2 in Experiment 1), where the interaction between adapt and test stimuli approached significance. See Table S2 for full results of statistical tests.

significant differences in adaptation effects across different adapting stimuli, and for significant interactions between adaptation and test stimulus in the adaptation effects (see Methods for details). The results of these statistical tests are shown in Table S2.

For BY/RG adaptation (Experiment 1, Fig. 4A) there was a tendency for within-stimulus adaptation to be greater than cross-stimulus adaptation across all ROIs, but this difference was only significant in area LO for the RG test, where RG adaptation produced greater signal loss than BY adaptation. In area VO2, the interaction between adapting and test stimuli approached significance ($p = 0.09$), and the interaction was in the direction of greater within-stimulus than cross-stimulus adaptation.

For BY/Ach adaptation (Experiment 2, Fig. 4B) both within-stimulus and cross-stimulus adaptation effects were similar and no differences or interactions reached statistical significance. Interestingly, for the ROIs that showed the greatest differences (hV4, VO1 and VO2), the trend was for greater cross-stimulus adaptation than within-stimulus adaptation, with no trend in the direction of selective adaptation. This complete lack of selectivity between BY and Ach responses is surprising and contrasts to previous results for RG/Ach stimuli in which selectivity (significantly greater within-stimulus adaptation than cross-stimulus adaptation) emerged for RG stimuli in ventral areas hV4 and VO (Mullen et al., 2015). Mullen et al. (2015) also found that in dorsal areas hMT+ and V3A, there was a trend for Ach selectivity from RG contrast although the difference between within- and cross-stimulus adaptation did not reach significance. These results implied the presence of separable responses to the RG and Ach contrasts in these regions, something that is not apparent for BY/Ach responses.

To test whether the lack of selective adaptation effects might reflect a low overall amplitude of adaptation (i.e. a floor effect), we repeated the analyses shown in Fig. 4 using only half the data. We selected those

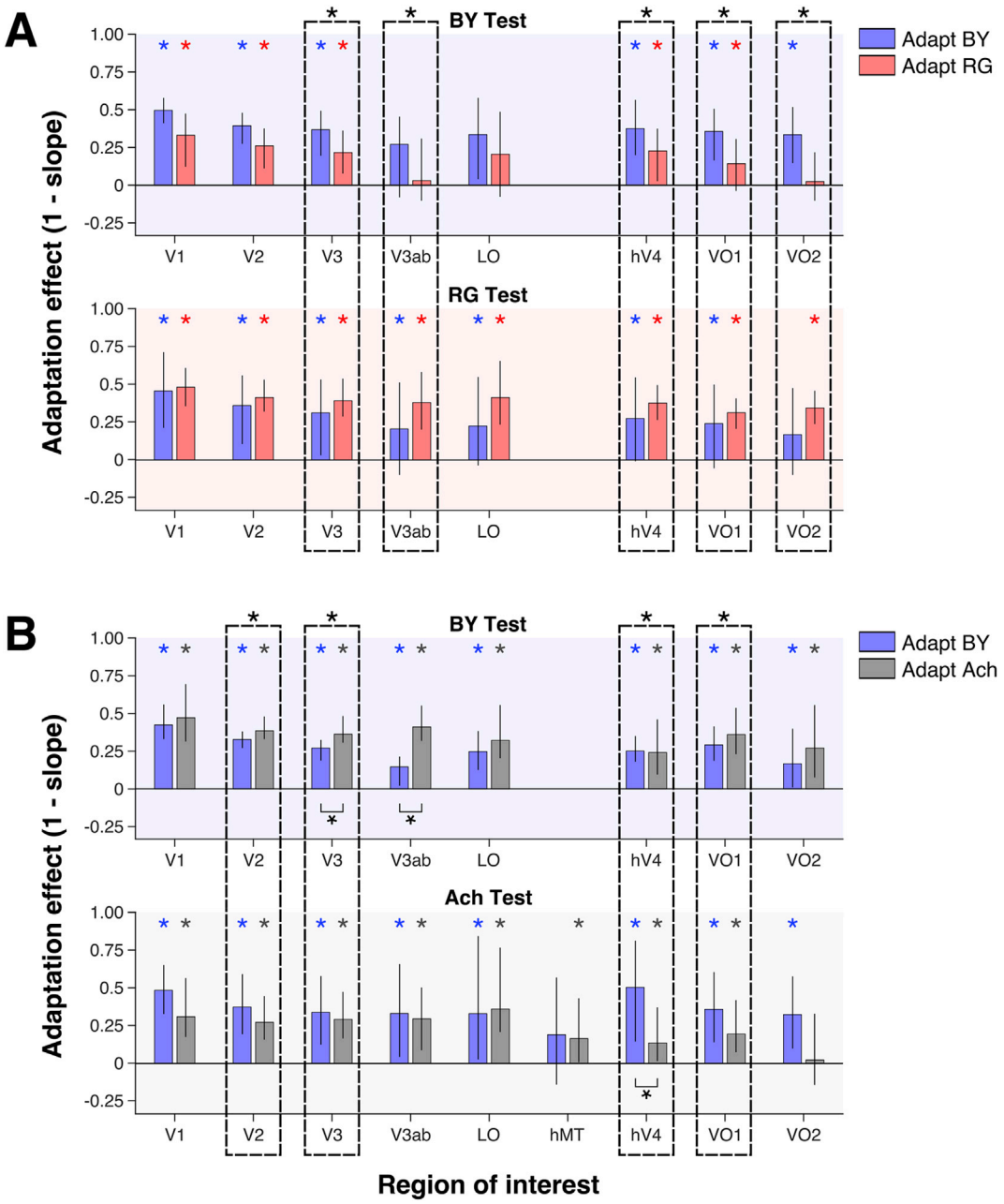

Fig. 5. Adaptation effects for the subset of participants (n = 6) with the largest adaptation effects: **(A)** Experiment 1, for the BY and RG stimuli and **(B)** Experiment 2, for the BY and stimuli. Plotting conventions as in Fig. 4. Boxes with dashed lines indicate cases where there was a significant interaction between adapt and test stimuli in the resultant adaptation effects ($p < 0.05$).

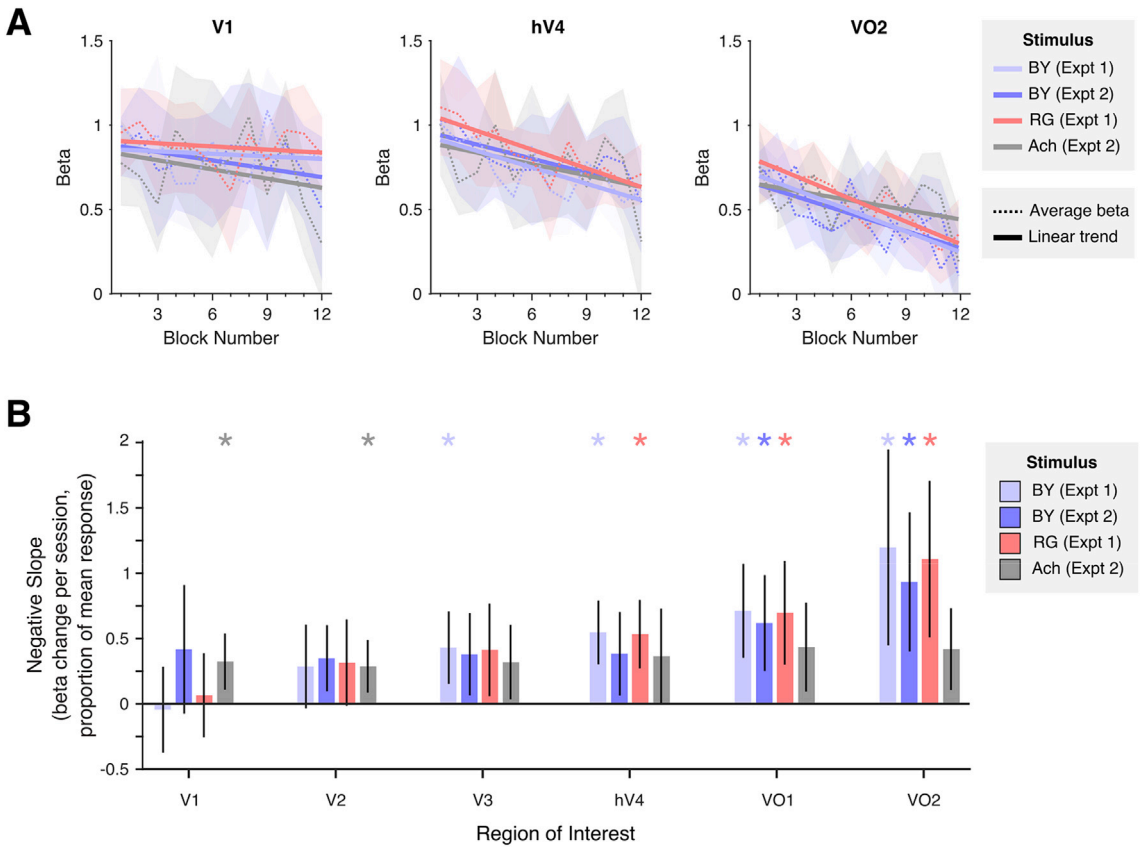

Fig. 6. Adaptation of the BOLD response across test stimulus presentations for early and ventral areas. **A**: For three example areas (V1, hV4 and VO2) we show the average response to each test stimulus following a blank (no adaptation baseline) across the 12 presentations. For each participant, we averaged responses to the 12 presentations across the two adaptation sessions. Lighter lines indicate the average response across participants ($n = 12$), with shaded error bars indicating the 95% confidence intervals of the between-subjects mean. Darker lines show the average slope of the lines of best fit that were fit to each participant's data separately. **B:** The average negative slope of the lines of best fit for each ROI, normalized for each participant by the ROI's mean response. Error bars indicating the 95% confidence interval of the between-subjects mean. Asterisks show those conditions where the average negative slope was significantly above zero ($q < 0.05$, *t*-test, FDR corrected).

participants ($n = 6$) with the largest adaptation effects when averaged across within- and cross-stimulus adaptation and asked whether a pattern of stimulus-selective adaptation emerged when the adaptation effects were larger in magnitude. The results of this control analysis are shown in Fig. 5. For both Experiments 1 and 2, there were a number of ROIs that showed selective adaptation in this control analysis, although these effects went in different directions across the two experiments, consistent with the main results. For the RG/BY pairs, the trend towards selectivity we observed in the main results manifested as significant interactions for areas V3, V3A/B, hV4, VO1 and VO2, where within-stimulus adaptation exceeded cross-stimulus adaptation in each case. However, for the BY/Ach pairs, the significant interactions that emerged for ROIs V2, V3, hV4 and VO1 were all in the opposite direction, that is, for greater cross-stimulus than within-stimulus adaptation.

3.2. Longer-term fMRI adaptation effects

We also tested whether there was evidence for adaptation over a longer time scale in our fMRI data. In the main results (Fig. 4), we were testing for differences in the response to a test stimulus following 12 s of an adapting stimulus compared with 12 s of a blank screen (i.e. mean gray). This comparison is insensitive to any changes in response that accumulate between runs, or across different presentations of the test stimulus within a run. To test for longer-term adaptation effects, we considered the average response to each test stimulus across all presentations within a session. For this analysis we included only those test stimulus presentations that followed a blank adaptation period, which gave 12 test stimulus presentations per session.

For each test stimulus, the BOLD response tended to decrease or remain steady with presentation number, as shown in Fig. 6 for early and ventral visual areas (see Figure S2 for dorsal areas V3A/B, LO and hMT+). The BY stimuli in Experiments 1 and 2 resulted in fairly similar patterns of results, despite the different participants and different alternate stimuli (RG vs Ach) in these experiments.

Interestingly, this slow decrease was of greater magnitude for higher level cortical areas tested than for lower ones. V1 showed virtually no longer-term adaptation, while V3A/B, hV4, VO1 and VO2 showed the highest levels of longer-term adaptation. Since area hMT+ had low mean responses to chromatic stimuli, the normalized slopes had very high variability across participants. For this reason, we excluded data from area hMT+ when performing ANOVAs. For the remaining 8 ROIs, a repeated measures ANOVA for BY/RG data (Expt 1) revealed a significant main effect of ROI ($p = 0.004$, $F_{(2.3,\ 24.8)} = 6.65$, $\eta_p^2 = 0.377$),[2] but no significant difference between BY/RG stimuli ($p = 0.98$, $F_{(1,11)} < 0.01$, $\eta_p^2 < 0.001$), nor an interaction between ROI and stimulus ($p = 0.81$, $F_{(2.4,\ 26.3)} = 0.26$, $\eta_p^2 = 0.023$)[1]. Across areas in the early and later ventral pathway (those shown in Fig. 6: V1, V2, V3, hV4, VO1 and VO2), there were significant linear trends in adaptation for BY stimuli ($p = 0.02$, $F_{(1,11)} = 7.59$, $\eta_p^2 = 0.408$) and for RG stimuli ($p = 0.01$, $F_{(1,11)} = 9.60$, $\eta_p^2 = 0.466$). For BY/Ach data (Expt 2), a repeated measures ANOVA did not reveal significant main effects of ROI ($p = 0.20$, $F_{(1.5,\ 16.6)} = 1.81$, $\eta_p^2 = 0.141$)[1] or stimulus ($p = 0.36$, $F_{(1,11)} = 0.93$, $\eta_p^2 = 0.078$), or their

[2] Degrees of freedom adjusted using a Greenhouse-Geisser epsilon to correct for violations of sphericity.

interaction ($p = 0.27$, $F_{(1.5,\ 16.8)} = 1.40$, $\eta_p^2 = 0.113$)[1]. The same trend analysis as above did not reveal significant trends for BY stimuli ($p = 0.25$, $F_{(1,11)} = 1.49$, $\eta_p^2 = 0.119$) or for Ach stimuli ($p = 0.18$, $F_{(1,11)} = 2.02$, $\eta_p^2 = 0.155$).

The fact that these longer-term adaptation effects tended to increase from V1 to higher order areas and depend on contrast type makes it unlikely that this slow timescale adaptation was related to adaptation of the BOLD response, to participant fatigue, or drifts in attention, which would affect all areas and/or contrast types similarly. Even though attention effects could be argued to particularly influence higher order areas (Sprague and Serences, 2013), robust attentional modulation of the BOLD response can occur in V1 (e.g. Jehee et al., 2011). We think variations in attention are unlikely to provide an account of our results: participants were engaged in a contrast discrimination task for each test stimulus throughout the entire session. Furthermore, there was evidence of a difference between chromatic and achromatic stimuli. Ach stimuli showed little longer-term adaptation, and this was relatively constant across ROIs. Where present, the differences across ROIs were driven by changes in longer-term adaptation for the chromatic stimuli (RG and BY). If a difference across areas were due to their different susceptibility to attentional effects, it is unlikely that this effect would differentially affect chromatic and achromatic stimuli.

3.3. Psychophysical adaptation effects

Psychophysical adaptation effects have demonstrated the existence of separable post-receptoral mechanisms. Reported results show selective adaptation for chromatic/achromatic pairs and between pairs of isoluminant chromatic stimuli isolating the L-M opponent and S-cone isolating mechanisms (Eskew, 2009; Krauskopf et al., 1982, 1986; Webster and Mollon, 1991, 1994). Based on this existing literature, we predicted that adaptation to our stimuli, modulated along the Ach, RG and BY mechanism-isolating directions, would be greatest for within-stimulus adaptation with little or no effect of cross-stimulus adaptation. Nonetheless, we explicitly tested whether our stimuli were also targeting these same separable mechanisms by measuring psychophysical adaptation effects for our stimuli at both threshold and suprathreshold levels. For these psychophysical experiments (Experiments 3 and 4) we used stimuli closely matched to those used in the fMRI experiments but used an adaptation protocol designed to be closer to that used in previous psychophysical work (including shorter test stimuli, and top-up adaptation between trials). Differences between the fMRI and psychophysical adaptation protocols are discussed below. Our subject cohort included four participants who had also taken part in fMRI experiments. We used a much larger cohort of subjects (n = 10) than used previously to ensure that our psychophysical data were unlikely to highly weighted by any individual's data. We did this in light of recent work (Gunther, 2014) demonstrating that there can be considerable individual variation in 'low-level' psychophysical measures which have traditionally been measured for smaller subject pools. The effects of adaptation on detection thresholds and on perceived contrast are shown in Fig. 7A and B respectively. Across both experiments and all test stimuli, we found that within-stimulus adaptation induced greater effects than cross-stimulus adaptation, broadly consistent with the existing literature (e.g. Krauskopf et al., 1982; Webster and Mollon, 1994).

For detection threshold (Fig. 7A), a 2-way repeated measures ANOVA of the $\log_2$-transformed effects of adaptor and test stimulus revealed significant main effects of adaptor ($p = 0.020$, $F_{(2,18)} = 4.89$, $\eta_p^2 = 0.352$),

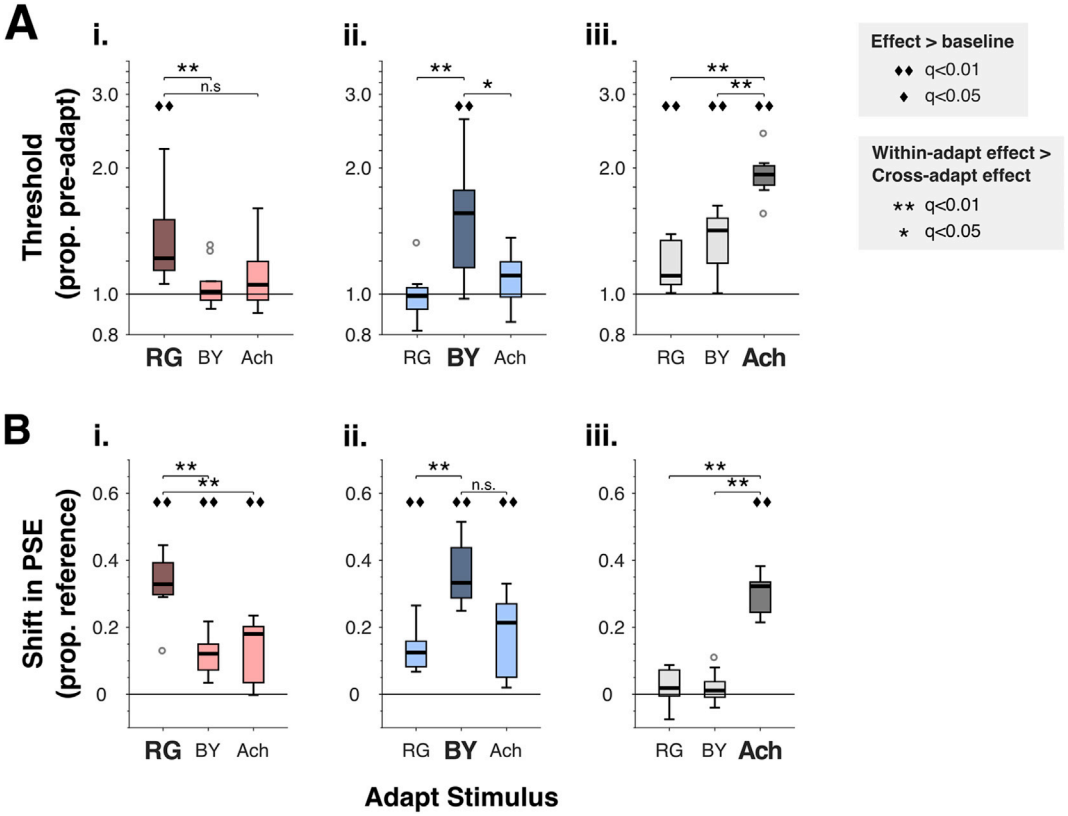

Fig. 7. Adaptation effects on detection thresholds (**A**) and perceived contrast (**B**) for RG (i), BY (ii) and Ach (iii) test stimuli. In **A**, each participant's post-adaptation shifts in detection thresholds are plotted as a proportion of their detection threshold prior to adaptation. In **B**, the post-adaptation shifts in apparent contrast are plotted, defined as the difference between the reference stimulus and the test stimulus judged to be of equal perceived contrast: the shift in point of subjective equality (PSE) is measured as contrast along the relevant color axis, as a proportion of the physical contrast of the reference stimulus. In all plots, the boxplots show the distributions of values across subjects ($n = 10$), including the median (thick black line), upper/lower quartiles (darker and lighter boxes for within- and cross-stimulus adaptation respectively) and outliers (gray circles).

and test stimulus ($p < 0.001$, $F_{(2,18)} = 14.23$, $\eta_p^2 = 0.613$), and a large, significant interaction between these effects ($p < 0.001$, $F_{(4,36)} = 41.32$, $\eta_p^2 = 0.821$). For Experiment 4 (Fig. 7B), we measured the post-adaptation shift in perceived contrast as the difference between the perceived contrast at the unadapted location and the adapted location. We performed a 4-way repeated measures ANOVA of the effects of adaptor stimulus, test stimulus, adaptor location (left or right) and reference location (same vs opposite to adaptor) on the post-adaptation shift in perceived contrast, and found a significant main effect of test stimulus ($p < 0.001$, $F_{(2,18)} = 17.87$, $\eta_p^2 = 0.665$), and a significant interaction between test and adapting stimuli ($p < 0.001$, $F_{(1.8,16.42)} = 67.69$, $\eta_p^2 = 0.883$)[1]. There was no significant main effect of adapting stimulus ($p = 0.08$, $F_{(2,18)} = 3.00$, $\eta_p^2 = 0.250$), adaptor location ($p = 0.22$, $F_{(1,9)} = 1.77$, $\eta_p^2 = 0.164$) or reference location ($p = 0.24$, $F_{(1,9)} = 1.62$, $\eta_p^2 = 0.152$). Neither was there a significant 3-way interaction between adaptor, test and adaptor location ($p = 0.70$, $F_{(1.8,16.6)} = 0.34$, $\eta_p^2 = 0.036$)[1] or between adaptor, test and reference location ($p = 0.51$, $F_{(1.45,13.0)} = 0.61$, $\eta_p^2 = 0.064$)[1]. Since there was no systematic pattern of variation with adaptor or reference location and these were not factors of interest, we show results for Experiment 4 averaged across these factors (Fig. 7) and focus on the effects of adapting and test stimulus.

Interestingly, we found patterns of cross-stimulus adaptation that differed between the two metrics used. We tested the statistical significance of the effects by performing a series of planned contrasts for the repeated measures ANOVAs, and applying a false discovery rate (FDR) criterion to correct for multiple comparisons (Benjamini and Hochberg, 1995). For each test stimulus, we asked whether each adapting stimulus produced a change in detection threshold or perceived contrast, and whether the within-stimulus adaptation effect differed from each cross-stimulus adaptation effect. The results of these are depicted in Fig. 7. When we measured detection thresholds, which are driven by the most sensitive neural responses and so are more likely to reveal separable neural mechanisms, achromatic test stimuli showed significant cross-adaptation by the chromatic adaptors (Fig. 7A iii), whereas chromatic test stimuli did not show any significant cross-stimulus adaptation (Fig. 7A i & ii) supporting the existence of selective neural responses to RG (Fig. 7Ai) and BY contrast (Fig. 7Aii). Conversely, when we measured suprathreshold perceived contrast, which we expect to also drive the less sensitive mechanisms and mechanisms dependent on combinations of responses, both chromatic test stimuli showed significant cross-stimulus adaptation by the other adaptors (Fig. 7B i & ii), whereas the Ach stimuli show no significant cross-stimulus adaptation (Fig. 7B iii), supporting highly selective achromatic responses but less selective responses to BY and RG contrast (Fig. 7Bi & ii).

These psychophysical cross-stimulus adaptation effects are also seen upon re-examination of the results of some previous studies. Previous work on interactions of this kind have focussed on the selective adaptation effects, rather than on whether there is any residual cross-stimulus adaptation. However, in Krauskopf et al. (1982) one of the two participants showed slightly elevated detection thresholds for achromatic tests following chromatic adaptation. Similarly, Webster and Mollon (1994) found that within the isoluminant plane, RG and BY adapting stimuli produced small cross-stimulus adaptation effects on perceived contrast, whereas RG adaptation with Ach tests produced little or no adaptation ($n = 3$). Here we build upon these previous results with a larger cohort ($n = 10$) with the majority ($n = 8$) completing both experiments and find that these small asymmetries in the interactions between cardinal directions are consistent across observers but vary across psychophysical measures.

3.4. Longer-term psychophysical adaptation effects

We tested for longer-term adaptation effects in our psychophysical data by considering the first and second halves of the data for each participant and asking whether aftereffects were greater in the second half of the data (after at least half an hour of adaptation) than in the first half. The results of this analysis for within-stimulus adaptation conditions are shown in Fig. 8. Since the participants included varied across conditions (as not all participants completed data for each condition in a single session), we used a series of paired-sample *t*-tests (with FDR correction for multiple comparisons) to evaluate whether there was a significant increase in adaptation effect for the later trials.

Unlike for the fMRI experiment, where there was no initial adaptation period (only 12s blocks), for the psychophysical experiments each run included an initial 60s of adaptation, with 2s of top-up adaptation before each trial. Nonetheless, here we also saw evidence that adaptation effects continued to accumulate across the session, with the within-stimulus adaptation effects for chromatic test stimuli recorded the second half of each session tending to be greater than those from the first half. Interestingly, this was not seen for the achromatic test, where adaptation effects were approximately equal for the first and second halves.

The results of cross-stimulus adaptation were more mixed (Figure S3), and there was only a single case (the effect of RG adaptor on BY detection threshold) where the adaptation effect increased from the first to the second half. However, since the cross-stimulus adaptation effects are much smaller than the within-stimulus adaptation there may be insufficient power to detect differences for these smaller effects.

4. Discussion

Motivated by previous fMRI results showing RG color selectivity in the ventral visual areas and clear psychophysical evidence supporting color selective adaptation, we tested the selectivity of adaptation between BY and Ach contrast and between the two chromatic axes, BY and RG. Our aim was to better characterize chromatic and achromatic selectivity across the different hierarchical stages of color processing in the visual cortex. Our results were surprising, however, in two key ways. First, our main finding showed a complete lack of stimulus-selective adaptation in the BOLD response between BY and Ach contrast at all cortical levels, with cross-stimulus adaptation (of the Ach test by BY contrast) even surpassing within-stimulus adaptation in ventral areas. Cross-stimulus adaption between the two color axes was also high, with only weak evidence for selective RG/BY color adaptation in ventral areas. Within those participants with the greatest adaptation effects (Fig. 5), cross-stimulus adaptation remained high, but there was greater evidence of selective RG/BY, but not BY/Ach, adaptation. Thus, a curious picture emerges of strong cross-stimulus adaptation occurring between BY/Ach contrast and between BY/RG contrast, and an absence of selective adaptation effects for BY/Ach contrast. Second, the psychophysical results, obtained using very similar stimuli, showed substantial differences between the fMRI and behavioral adaptation effects, with overall much greater stimulus selectivity in psychophysical adaptation despite some interesting differences between the threshold and suprathreshold behavioral metrics used. Our results suggest that a re-evaluation of fMRI adaptation in the cortex in relation to behavioral data is required, along with a keener understanding of the BOLD response to BY contrast in the visual cortex.

4.1. Lack of stimulus-selectivity in fMRI adaptation

High cross-stimulus adaptation was also found in the early visual areas (V1-V3) in the previous study with RG/Ach stimuli (Mullen et al., 2015) and is consistent with a high proportion of neurons responding jointly to chromatic and achromatic stimuli (Hass and Horwitz, 2013; Shapley and Hawken, 2011). Moreover, in V1, neurons with significant non-linear interactions between S-cones and achromatic responses have been shown to enhance S-cone color responses (Horwitz et al., 2005), supporting cross-modal BY and Ach processing in V1. In the previous study, significant RG selectivity emerged in ventral areas, particularly VO (Mullen et al., 2015), whereas here for BY/Ach contrast we find strong cross-adaptation and an absence of selectivity in all areas, including the ventral ones. This may imply a greater segregation between Ach and RG

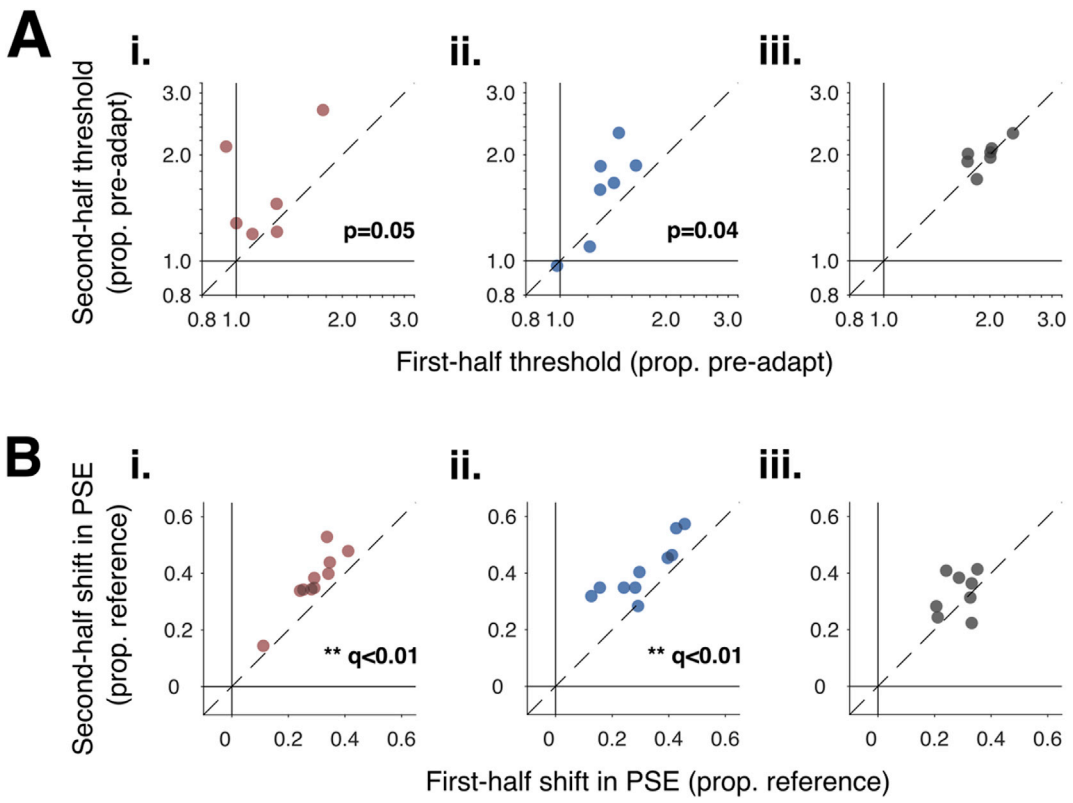

Fig. 8. Change in within-stimulus adaptation effects from first to second half of sessions from Experiments 3 (**A**) and 4 (**B**) for RG (i), BY (ii) and Ach (iii) test stimuli. For each condition we only included data from those participants who completed the condition in a single session of approximately 1 h ($n = 6$ or 7 for **A**, $n = 8$ or 10 for **B**). The results of paired-sample *t*-tests (lower right of relevant plots) are shown for those conditions where the adaptation effect in the second half of the session exceeded that in the first half (asterisks indicate the FDR-corrected results, *p*-values indicate the uncorrected *p*-value where $p < 0.05$ but did not reach the criterion for FDR correction at $q < 0.05$).

signals in ventral cortex than between BY and Ach or RG, however, this is not matched by the psychophysical results. At detection threshold, the absence of significant cross-adaptation implies the existence of neural mechanisms that respond selectively to RG contrast (Fig. 7Ai) and to BY contrast (Fig. 7Aii). At suprathreshold contrast levels, more akin to the BOLD conditions, the psychophysical responses to Ach contrast are highly selective. The BY and RG color responses have similar selectivities (Fig. 7Bi & ii), with both also showing significant cross-adaptation by the achromatic and the other chromatic contrast. Rather little is known about the organization of color responses in V4, and even less in VO, however, given the widely accepted specialization of both of these areas for color (Brouwer and Heeger, 2013; Roe et al., 2012; Tanigawa et al., 2010; Conway and Tsao, 2009; Lafer-Sousa et al., 2016), the unselective BY and Ach BOLD responses are surprising. Lastly, previous reports have shown surprisingly strong cortical BOLD responses to BY stimuli, greater than predicted from their threshold scaling (Kuriki et al., 2015; Mullen et al., 2007, 2008), and here we show that BY contrast also has an unexpectedly strongly influence on RG and Ach responses and vice versa.

Importantly, the lack of stimulus selectivity in the adaptation of BOLD responses cannot be simply attributed to a low level of adaptation (a floor effect), particularly in the case of BY/Ach adaptation. Data for those participants with the largest overall adaptation effects (Fig. 5) show some evidence of selective adaptation of RG/BY stimuli, but no evidence of selectivity for BY/Ach adaptation. Furthermore, even for this subset of high-adapting participants there are significant cross-stimulus adaptation effects. Our protocol for BOLD adaptation was designed around the constraints of a fMRI design; in order to obtain good separation of the responses to adaptor and test, we used test stimuli that were much longer (18 s) than in a typical psychophysical design. Additionally, to avoid comparisons across early and late periods in the fMRI session, we interleaved no adaptation and adaptation blocks throughout the session, whereas psychophysical designs (including here for Experiments 3 and 4) typically measure a no adaptation baseline before any adaptation has occurred. For these reasons, BOLD adaptation effects could be of lower overall amplitude than psychophysical effects. Despite this, we found robust BOLD adaptation effects across all areas. The lack of stimulus-selectivity was not due to a lack of within-stimulus adaptation, but due to a surprising degree of cross-stimulus adaptation in each case. These strong cross-stimulus adaptation effects occurred despite the psychophysical evidence for selective mechanisms, and despite the fact that the same protocol had previously revealed selective adaptation in some regions for some stimulus combinations (Mullen et al., 2015). Nevertheless, we cannot rule out that different stimuli or protocols will potentially yield different results, particularly for an event-related fMRI design with timing closer to a typical psychophysical protocol. We think the lack of selectivity is less likely to change for the Ach/BY pairs, which show no evidence for selectivity, but might potentially increase in the RG/BY pairings, which show a trend for selectivity.

Why, then, are there such strong cross-stimulus adaptation effects, especially for stimulus pairings that include the BY stimuli (BY/Ach and RG/BY)? There are previous instances where fMRI adaptation has failed to reveal selectivity when expected: for a discussion of such results see (Krekelberg et al., 2006). In V1, both Boynton and Finney (2003) and Murray et al. (2006) found strong fMRI adaptation to oriented gratings, but a surprising lack of selectivity to orientation, despite substantial evidence of orientation sensitivity and orientation-selective adaptation in V1 (e.g. Carandini et al., 1998; Hubel and Wiesel, 1959). Fang et al. (2005) suggested that orientation-selective adaptation effects in V1 may vary with stimulus timing (although see Kourtzi et al., 2003 versus Murray et al., 2006). Our adapting stimuli exceeded the long-term adaptation condition of Fang et al. (2005), making it unlikely that stimulus timing accounts for our lack of selective adaptation. In their

review of fMRI adaptation (Krekelberg et al., 2006) note that these inconsistencies in fMRI adaptation results do not undermine the interpretation where selective adaptation occurs, but mean that null results cannot be taken to mean a lack of stimulus selectivity. They also note that instances of absent selective fMRI adaptation in V1 might be partly attributable to higher order areas adapting more easily than earlier ones. Our results are a particularly striking example of a failure to find selective fMRI adaptation, which occurs despite strong adaptation effects and a long adapting stimulus, even for higher areas (e.g. VO1 and VO2).

We have no direct evidence on what causes the greater level of cross adaptation in the BOLD experiments compared to behavior. Murray et al. (2006) argue that BOLD adaptation effects may be driven by adaptation of the haemodynamic response, rather than adaptation of the neural signals. However, this account is inconsistent with recent work on the effects of adaptation on neurovascular-coupling which suggest that BOLD measurements will tend to underestimate, rather than overestimate, neural adaptation effects (Larsson et al., 2015; Moradi and Buxton, 2013). It is also inconsistent with our results showing evidence for selectivity for some contrast pairs.

More plausibly, we speculate that the strong cross-stimulus adaptation of the BOLD response may be related to the fact that the BOLD response reflects the activity of both driver neurons and the normalization pool, including non-spiking activity (Logothetis, 2008). In general terms, if the BOLD response reflects the combined activity of both excitatory (driver) and inhibitory (normalization) mechanisms, then BOLD adaptation may reflect the *summed* effects of adaptation on driver and normalization mechanisms, whereas the spiking output and perception would correspond more closely to the effects of adaptation on the *ratio* or balance between these opposing influences. In this way, BOLD adaptation effects may be dissociated from perceptual effects where the effect of adaptation on the combined activity of driver and normalization mechanisms is different to the effect on the balance between these mechanisms.

The notion that adaptation affects normalization mechanisms is supported by work from single-unit electrophysiology. Tailby et al. (2008) demonstrated for macaque V1 cells that chromatic adaptation effects could not be accounted for by adaptation of a linear receptive field alone, but that their data were well described by a model that also included an adaptable normalization pool, with preferred chromaticity that was often different from that of the linear receptive field. Furthermore, Tailby et al. (2008) found that across cells the best-fitting models included a normalization pool that was very broadly tuned for chromaticity. For the RG/BY data from Experiment 1, the cross-stimulus adaptation effects may reflect adaptation of a normalization pool is that is very broadly tuned for chromaticity and/or has a different preferred chromaticity to the linear receptive field, while there is a much lower effect of adaptation on the resultant spiking output. While the results and modelling of (Tailby et al., 2008) only include the equiluminant plane, a similar principle may apply to BY/Ach adaptation. Note that this speculative account does not explain how cross-stimulus could result in even greater adaptation effects than within-stimulus adaptation.

The notion that fMRI adaptation reflects adaptation of both excitatory and inhibitory mechanisms is also discussed in a recent review (Larsson et al., 2015) where adaptation of a suppressive surround was proposed to account for fMRI adaptation to spatially displaced stimuli (Larsson and Harrison, 2015). Interestingly, Larsson et al. (2015) predict that where adaptation of normalising surround mechanisms contributes to BOLD adaptation, reducing stimulus size should reduce the adaptation of the surround. Our findings suggest that chromatic contrast adaptation would be an ideal stimulus for testing this prediction.

4.2. Psychophysical effects of adaptation

In line with previous psychophysical work (Krauskopf et al., 1982, 1986; Webster and Mollon, 1991, 1994), we found that within-stimulus adaption evoked the greatest adaptation effects (Fig. 7) but, interestingly, we find different patterns of interactions for threshold and suprathreshold contrast measurements. The detection threshold metric, revealing the responses of the most sensitive mechanisms, supports the separation of the two chromatic responses (Fig. 7Ai & ii), however, the residual but significant cross-adaption of the Ach test by color is surprising (Fig. 7Aiii). For suprathreshold contrast-matching both chromatic test stimuli show evidence of more interaction with other axes (Fig. 7Bi & ii), which could be related to the suprathreshold stimuli evoking responses in broadly-tuned mechanisms in the isoluminant plane, preferring non-cardinal color directions (Webster and Mollon, 1994). However, the Ach suprathreshold response is the most selective with no significant cross-adaptation by color (Fig. 7Biii): this greater selectivity at suprathreshold contrasts is an effect in the opposite direction to that for color stimuli. These asymmetries are similar to those for masking (Kim and Mullen, 2016) and consistent with populations of neurons responding selectively to Ach contrast (Johnson et al., 2004). Nevertheless, an effect of chromatic adaptation on Ach at detection threshold implies that the most sensitive luminance mechanisms may retain some sensitivity to color contrast.

4.3. Slow adaptation increases for higher-level areas in visual cortex

In addition to the main BOLD adaptation effects reported above, we also found a general decrease in the BOLD response to test stimuli across the session of ~1 h (Fig. 6). If this decrease in BOLD across the session reflects a slow adaptation effect, then the increase in adaptation magnitude from V1 to higher order areas is broadly consistent with evidence that these areas have increasing windows of temporal integration (Gauthier et al., 2012; Hasson et al., 2008; Mattar et al., 2016; Noguchi et al., 2004). However, a key difference between these previous results and the trends we observe is the scale: in previous studies the longest timescale considered was ~30s (Hasson et al., 2008), whereas we saw trends across the entire session (~1h). In terms of achromatic contrast adaptation, Gardner et al. (2005) found time constants in the order of tens of seconds for a BOLD response to a static Ach checkerboard.

A further suggestion that chromatic contrast adaptation is accumulating over this long timescale comes from the psychophysical data (Fig. 8). Interestingly, this longer-term adaptation was present for chromatic stimuli but not achromatic stimuli, similar to the BOLD effect that was strongest for chromatic stimuli. Previous work on the time-course of chromatic contrast adaptation is sparse: Krauskopf et al. (1982) report that over the initial minute of adaptation, most of the desensitizing effect takes place over the first 15 s. Tregillus and Webster (2014) tested chromatic contrast adaptation across the course of 1 h and found that for three of four participants the changes in apparent contrast occurred within the first 10 min, with only one of four participants showing a steady buildup of adaptation across the hour.

Future work may identify whether adaptation effects across different timescales share a common mechanism or have different origins. Here, both the BOLD and psychophysical effects suggest that chromatic contrast adaptation may be greater than achromatic contrast adaptation at the 1h timescale.

Data availability

Data from fMRI experiments are freely available online from the Open Science Framework (DOI: https://doi.org/10.17605/OSF.IO/PK8N3). This online repository includes deidentified raw data from the fMRI experiments, details of the stimulus timing for each participant, and the AFNI code used to perform the analyses reported here.

Acknowledgements

This work was funded by Canadian Institutes of Health Research grants 153277 and 10819 to KTM and 228103 to RFH. We thank Michael Ferreira and the imaging technicians at the McConnell Brain Imaging

Center for their advice on fMRI protocols and their assistance with data collection. We also thank Asli Bese and Hannah Jin for their assistance with psychophysical data collection.

Appendix A. Supplementary data

Supplementary data to this article can be found online at https://doi.org/10.1016/j.neuroimage.2019.116032.

References

Benjamini, Y., Hochberg, Y., 1995. Controlling the false discovery rate: a practical and powerful approach to multiple testing. J. R. Stat. Soc. Ser. B Methodol. 57, 289–300.

Boynton, G.M., Finney, E.M., 2003. Orientation-specific adaptation in human visual cortex. J. Neurosci. Off. J. Soc. Neurosci. 23, 8781–8787.

Bradley, A., Zhang, X., Thibos, L., 1992. Failures of isoluminance caused by ocular chromatic aberrations. Appl. Opt. 31, 3657–3667.

Brainard, D.H., 1997. The psychophysics toolbox. Spat. Vis. 10, 433–436.

Brouwer, G.J., Heeger, D.J., 2013. Categorical clustering of the neural representation of color. J. Neurosci. 33, 15454–15465.

Carandini, M., Movshon, J.A., Ferster, D., 1998. Pattern adaptation and cross-orientation interactions in the primary visual cortex. Neuropharmacology 37, 501–511.

Chang, D.H.F., Hess, R.F., Mullen, K.T., 2016. Color responses and their adaptation in human superior colliculus and lateral geniculate nucleus. Neuroimage 138, 211–220.

Conway, B.R., Tsao, D.Y., 2009. Color-tuned neurons are spatially clustered according to color preference within alert macaque posterior inferior temporal cortex. Proc. Natl. Acad. Sci. U.S.A. 106, 18034–18039.

Cottaris, N.P., 2003. Artifacts in spatiochromatic stimuli due to variations in preretinal absorption and axial chromatic aberration: implications for color physiology. J. Opt. Soc. Am. -Opt. Image Sci. Vis. 20, 1694–1713.

Cox, R.W., 1996. AFNI: software for analysis and visualization of functional magnetic resonance neuroimages. Comput. Biomed. Res. 29, 162–173.

Dale, A.M., Fischl, B., Sereno, M.I., 1999. Cortical surface-based analysis. I: segmentation and surface reconstruction. Neuroimage 9, 179–194.

Engel, S.A., 2005. Adaptation of oriented and unoriented color-selective neurons in human visual areas. Neuron 45, 613–623.

Engel, S.A., Furmanski, C.S., 2001. Selective adaptation to color contrast in human primary visual cortex. J. Neurosci. 21, 3949–3954.

Engel, S.A., Rumelhart, D.E., Wandell, B.A., Lee, A.T., Glover, G.H., Chichilnisky, E.J., Shadlen, M.N., 1994. fMRI of human visual cortex. Nature 369, 525.

Eskew, R.T., 2009. Higher-order color mechanisms: a critical review. Vis. Res. 49, 2686–2704.

Fang, F., Murray, S.O., Kersten, D., He, S., 2005. Orientation-tuned FMRI adaptation in human visual cortex. J. Neurophysiol. 94, 4188–4195.

Farnsworth, D., 1957. The Farnsworth-Munsell 100-hue Test for the Examination of Color Discrimination.

Gardner, J.L., Sun, P., Waggoner, R.A., Ueno, K., Tanaka, K., Cheng, K., 2005. Contrast adaptation and representation in human early visual cortex. Neuron 47, 607–620.

Gauthier, B., Eger, E., Hesselmann, G., Giraud, A.-L., Kleinschmidt, A., 2012. Temporal tuning properties along the human ventral visual stream. J. Neurosci. Off. J. Soc. Neurosci. 32, 14433–14441.

Goddard, E., Mannion, D.J., McDonald, J.S., Solomon, S.G., Clifford, C.W.G., 2011. Color responsiveness argues against a dorsal component of human V4. J. Vis. 11 (3), 1–21.

Gunther, K.L., 2014. Non-cardinal color mechanism strength differs across color planes but not across subjects. J. Opt. Soc. Am. A Opt. Image Sci. Vis. 31, A293–A302.

Hass, C.A., Horwitz, G.D., 2013. V1 mechanisms underlying chromatic contrast detection. J. Neurophysiol. 109, 2483–2494.

Hasson, U., Yang, E., Vallines, I., Heeger, D.J., Rubin, N., 2008. A hierarchy of temporal receptive windows in human cortex. J. Neurosci. 28, 2539–2550.

Horwitz, G.D., Chichilnisky, E.J., Albright, T.D., 2005. Blue-yellow signals are enhanced by spatiotemporal luminance contrast in macaque V1. J. Neurophysiol 93, 2263–2278. https://doi.org/10.1152/jn.00743.2004.

Hubel, D.H., Wiesel, T.N., 1959. Receptive fields of single neurones in the cat's striate cortex. J. Physiol. 148, 574–591.

Huk, A., Dougherty, R., Heeger, D., 2002. Retinotopy and functional subdivision of human areas MT and MST. J. Neurosci. 22, 7195–7205.

Ishihara, S., 1990. Ishihara's Tests for Color-Blindness, 38 plate ed. Kyoto: Kanehara, Shuppan Co. Ltd., Tokyo.

Jehee, J.F.M., Brady, D.K., Tong, F., 2011. Attention improves encoding of task-relevant features in the human visual cortex. J. Neurosci. 31, 8210–8219.

Johnson, E.N., Hawken, M.J., Shapley, R., 2004. Cone inputs in macaque primary visual cortex. J. Neurophysiol. 91, 2501–2514.

Kim, Y.J., Mullen, K.T., 2016. Effect of overlaid luminance contrast on perceived color contrast: shadows enhance, borders suppress. J. Vis. 16, 15.

Kleiner, M., Brainard, D., Pelli, D.G., 2007. What's New in Psychtoolbox-3? Perception, vol. 36. ECVP Abstract Supplement.

Kourtzi, Z., Tolias, A.S., Altmann, C.F., Augath, M., Logothetis, N.K., 2003. Integration of local features into global shapes: monkey and human FMRI studies. Neuron 37, 333–346.

Krauskopf, J., Williams, D.R., Heeley, D.W., 1982. Cardinal directions of color space. Vis. Res. 22, 1123–1131.

Krauskopf, J., Williams, D.R., Mandler, M.B., Brown, A.M., 1986. Higher order color mechanisms. Vis. Res. 26, 23–32.

Krekelberg, B., Boynton, G.M., van Wezel, R.J.A., 2006. Adaptation: from single cells to BOLD signals. Trends Neurosci. 29, 250–256.

Kuriki, I., Sun, P., Ueno, K., Tanaka, K., Cheng, K., 2015. Hue selectivity in human visual cortex revealed by functional magnetic resonance imaging. Cerebr. Cortex 25, 4869–4884.

Lafer-Sousa, R., Conway, B.R., Kanwisher, N.G., 2016. Color-biased regions of the ventral visual pathway lie between face- and place-selective regions in humans, as in macaques. J. Neurosci. 36, 1682–1697.

Larsson, J., Harrison, S.J., 2015. Spatial specificity and inheritance of adaptation in human visual cortex. J. Neurophysiol. 114, 1211–1226.

Larsson, J., Heeger, D.J., 2006. Two retinotopic visual areas in human lateral occipital cortex. J. Neurosci. 26, 13128–13142.

Larsson, J., Solomon, S.G., Kohn, A., 2015. fMRI Adaptation Revisited. Cortex.

Logothetis, N.K., 2008. What we can do and what we cannot do with fMRI. Nature 453, 869–878.

Mattar, M.G., Kahn, D.A., Thompson-Schill, S.L., Aguirre, G.K., 2016. Varying timescales of stimulus integration unite neural adaptation and prototype formation. Curr. Biol. CB 26, 1669–1676.

Michna, M.L., Yoshizawa, T., Mullen, K.T., 2007. S-cone contributions to linear and non-linear motion processing. Vis. Res. 47, 1042–1054.

Moradi, F., Buxton, R.B., 2013. Adaptation of cerebral oxygen metabolism and blood flow and modulation of neurovascular coupling with prolonged stimulation in human visual cortex. Neuroimage 82, 182–189.

Mullen, K.T., 1985. The contrast sensitivity of human colour vision to red-green and blue-yellow chromatic gratings. J. Physiol. 359, 381–400.

Mullen, K.T., Dumoulin, S.O., McMahon, K.L., de Zubicaray, G.I., Hess, R.F., 2007. Selectivity of human retinotopic visual cortex to S-cone-opponent, L/M-cone-opponent and achromatic stimulation. Eur. J. Neurosci. 25, 491–502.

Mullen, K.T., Dumoulin, S.O., Hess, R.F., 2008. Color responses of the human lateral geniculate nucleus: selective amplification of S-cone signals between the lateral geniculate nucleno and primary visual cortex measured with high-field fMRI. Eur. J. Neurosci. 28, 1911–1923.

Mullen, K.T., Thompson, B., Hess, R.F., 2010. Responses of the human visual cortex and LGN to achromatic and chromatic temporal modulations: an fMRI study. J. Vis. 10, 13.

Mullen, K.T., Chang, D.H.F., Hess, R.F., 2015. The selectivity of responses to red-green colour and achromatic contrast in the human visual cortex: an fMRI adaptation study. Eur. J. Neurosci. 42, 2923–2933.

Murray, S.O., Olman, C.A., Kersten, D., 2006. Spatially specific FMRI repetition effects in human visual cortex. J. Neurophysiol. 95, 2439–2445.

Noguchi, Y., Inui, K., Kakigi, R., 2004. Temporal dynamics of neural adaptation effect in the human visual ventral stream. J. Neurosci. Off. J. Soc. Neurosci. 24, 6283–6290.

Pelli, D.G., 1997. The VideoToolbox software for visual psychophysics: transforming numbers into movies. Spat. Vis. 10, 437–442.

Roe, A.W., Chelazzi, L., Connor, C.E., Conway, B.R., Fujita, I., Gallant, J.L., Lu, H., Vanduffel, W., 2012. Toward a unified theory of visual area V4. Neuron 74, 12–29.

Saad, Z.S., Ropella, K.M., Cox, R.W., DeYoe, E.A., 2001. Analysis and use of FMRI response delays. Hum. Brain Mapp. 13, 74–93.

Saad, Z.S., Reynolds, R.C., Argall, B., Japee, S., Cox, R.W., 2004. SUMA: an interface for surface-based intra- and inter-subject analysis with AFNI. Proc IEEE Int. Symp. Biomed. Imaging Macro Nano 1510–1513.

Sereno, M.I., Dale, A.M., Reppas, J.B., Kwong, K.K., Belliveau, J.W., Brady, T.J., Rosen, B.R., Tootell, R.B., 1995. Borders of multiple visual areas in humans revealed by functional magnetic resonance imaging. Science 268, 889–893.

Shapley, R., Hawken, M.J., 2011. Color in the cortex: single- and double-opponent cells. Vis. Res. 51, 701–717.

Sprague, T.C., Serences, J.T., 2013. Attention modulates spatial priority maps in the human occipital, parietal and frontal cortices. Nat. Neurosci. 16, 1879–1887.

Tailby, C., Solomon, S.G., Dhruv, N.T., Lennie, P., 2008. Habituation reveals fundamental chromatic mechanisms in striate cortex of macaque. J. Neurosci. 28, 1131–1139.

Tanigawa, H., Lu, H.D., Roe, A.W., 2010. Functional organization for color and orientation in macaque V4. Nat. Neurosci. 13, 1542–1548.

Tregillus, K., Webster, M.A., 2014. Dynamics of color contrast adaptation. J. Opt. Soc. Am. -Opt. Image Sci. Vis. 31, A314–A321.

Wandell, B.A., Brewer, A.A., Dougherty, R.F., 2005. Visual field map clusters in human cortex. Phil. Trans. R. Soc. Lond. Ser. B Biol. Sci. 360, 693–707.

Webster, M.A., Mollon, J.D., 1991. Changes in colour appearance following post-receptoral adaptation. Nature 349, 235–238.

Webster, M.A., Mollon, J.D., 1994. The influence of contrast adaptation on color appearance. Vis. Res. 34, 1993–2020.